Satellite observation highlights of the 2010 Russian Wildfires

Jacquelyn C. Witte[1], Anne R. Douglass[2], Bryan N. Duncan[2], Arlindo da Silva[2], and Omar Torres[2]

[1]Science Systems and Applications Inc. Lanham, MD, 20703, USA
[2]NASA Goddard Space Flight Center, Code 613.3, Greenbelt, MD 20771, USA

From mid-June 2010 through August western Russia experienced an unprecedented heat wave characterized by prolonged high temperatures (~ 40degC) and drought conditions. The heat wave set-up the ideal meteorological conditions for an unprecedented wildfire event. Plumes of thick smoke and burning pollution products were reported over highly populated regions including the capitol city of Moscow. The negative human and economic impacts were severe and extensively covered by the local and international media.

Our study took advantage of the large complement of NASA's Earth Observing System (EOS) sensors to track and quantify the source of the thick smoke and wildfire byproducts, such as carbon monoxide (CO), which settled over Moscow and nearby cities. A typical tracer of carbonaceous (or smoke) aerosols produced from wildfires smoke aerosols is the Aerosol Index (AI) that is measured by the Ozone Monitoring Instrument (OMI) on-board the Aura satellite. Over Moscow, OMI measured unprecedented levels of smoke aerosols between the end of July and mid-August that were an order of magnitude higher than previous summers going back to the earliest record in 2005. Likewise, CO, measured by the Atmospheric Infrared Sounder (AIRS) on-board Aqua, showed exceptionally high levels over Moscow. Previous summers going back to 2003 typically have an average CO concentration of 20×10^{17} molecules/cm^2. However, during the peak of the 2010 wildfires, CO averaged around 35×10^{17} molecules/cm^2. To put this wildfire event into perspective, the magnitude of the CO we observed over Moscow was equivalent to the 2006 El Nino wildfire event over Indonesia where some of the most intense wildfires have been documented.

Using the MODIS fire count data on-board the Aqua and Terra satellites, we observed numerous wildfires throughout western Russia and Eastern Europe that raged for almost three weeks between the end of July and mid-August. During this time period air-parcel back-trajectories initiated from Moscow traced the origin of the enhanced smoke pollution from wildfires raging in the southeast. The MODIS Fire Radiative Power (FRP) product measured very intense of the fires clustered in that same region and AIRS CO was also historically high.

Satellite observation highlights of the 2010 Russian Wildfires

Jacquelyn C. Witte[1], Anne R. Douglass[2], Bryan N. Duncan[2], Arlindo M. da Silva[2], and Omar Torres[2]

[1]Science Systems and Applications Inc. Lanham, MD, 20703, USA
[2]NASA Goddard Space Flight Center, Code 613.3, Greenbelt, MD 20771, USA

Abstract

From late-July through mid-August 2010, wildfires raged in western Russia. The resulting thick smoke and biomass burning products were transported over the highly populated Moscow city and surrounding regions, seriously impairing visibility and affecting human health. We demonstrate the uniqueness of the 2010 Russian wildfires by using satellite observations from NASA's Earth Observing System (EOS) platforms. Over Moscow and the region of major fire activity to the southeast, we calculate unprecedented increases in the MODIS fire count record of 178 %, an order of magnitude increase in the MODIS fire radiative power (308%) and OMI absorbing aerosols (255%), and a 58% increase in AIRS total carbon monoxide (CO). The exceptionally high levels of CO are shown to be of comparable strength to the 2006 El Niño wildfires over Indonesia. Both events record CO values exceeding 30×10^{17} molec-cm^{2}.

1. Introduction

Forest fires are both a source and sink of carbon, releasing carbon dioxide (CO_2) and CO to the atmosphere while burning, and removing of CO_2 during post-fire re-growth, thus playing an important role in the global carbon cycle [*Olson et al.,* 1983; *Crutzen and Andreae*, 1990; *Kasischke et al.,* 2005]. Russia includes approximately 30% of the world's total forested area, and forest fires are common [*Alimov et al.,* 1989]. Despite improvements in spatio-temporal coverage of fire events due to satellite monitoring, the behavior of forest ecosystems under fire conditions remains uncertain [*Mottram et al.*, 2005]. Forecasting the influence of forest fires on regional and global scales remains a challenge.

The 2010 Russian wildfires was an unprecedented forest fire event that spread dangerously towards populated regions, significantly impacting human health and livelihood. Media coverage was extensive and socio-economic statistics and impacts are readily available in the on-line literature. A blocking high-pressure system over western Russia and parts of Eastern Europe resulted in anomalously high temperatures and dry conditions in July and August 2010 [*Lau and Kim*, 2010]. Our study will show that from late-July through mid-August the circulation produced by the blocking event transported heavy wildfire smoke and burning byproducts, such as CO, over Moscow and surrounding regions. Consequently, the city experienced impaired visibility and unhealthy levels of smoke and smog, compounded by local pollution sources. We use observations of fire activity, smoke, and CO from several sensors on NASA's EOS platforms including Aura, Aqua, and Terra to show that the 2010 Russian wildfires are unique in the observing records of these sensors.

The next section describes the observations used in this study, followed by the analyses in section 3. Included is an overview of the regional meteorological conditions from daily radiosondes at various locations in the western Russia, including Moscow. We also compare the 2010 Russian wildfires with the 2006 El Niño wildfires in Indonesia.

2. Satellite Data

2.1 Active Fire Counts and Fire Radiative Power

Active fire count data are taken from the Moderate Resolution Imaging Spectroradiometer (MODIS) instruments on NASA's Terra and Aqua satellites that were launched in December 1999 and May 2002, respectively. The Level 2 active fires products MOD14 (Terra) and MYD14 (Aqua) have a pixel size of 1 km^2 at nadir covering an area of 2340×2030 km in the across- and along-track directions, respectively. The fire detection algorithm is described in *Giglio et al.*, [2003] and has been shown to provide useful information about the spatial and temporal dynamics of fire activity [*Giglio et al, 2006* and references therein]. The fire detection strategy is based on absolute detection of a fire (when the fire strength is sufficient to detect), and on detection relative to its background (to account for variability of the surface temperature and reflection by sunlight). The Fire Radiative Power (FRP, in Megawatts) measures the radiant heat output of the detected fires. *Kaufman et al.* [1996] developed an empirical non-linear relationship between the MODIS mid-infrared channel brightness temperatures at an active fire pixel, and the fire FRP over all wavelengths.

2.2 UV Aerosol Index

The Dutch-Finnish OMI instrument is a nadir-viewing moderate resolution UV/Vis spectrometer on NASA's Aura satellite, launched on July 2004 into a sun-synchronous orbit with an equator crossing-time of 13:38 in the ascending node. OMI has a full cross-track swath of 2600 km, containing 60 pixels ranging from 15×30 km^2 at nadir to 42×162 km^2 at the edge of the swath. The OMAERUV aerosol algorithm uses the radiances measured at 354 and 388 nm to retrieve the UV Aerosol Index (UVAI). *Torres et al.* [2007] and references therein describe the algorithm that was originally developed for TOMS (Total Ozone Mapping Spectrometer). All UVAI data have been filtered for the row anomalies that have affected the Level 2 data since 2007. Detailed information on the OMI row anomaly can be found at http://www.knmi.nl/omi/research/product/rowanomaly-background.php.

2.3 Total Column CO

Aqua's Atmospheric Infrared Sounder (AIRS) is a cross-track scanning grating spectrometer that provides total column CO (CO_{TC}) data with a nadir 45 km field of view across a 1650 km swath [*Aumann et al.,* 2003]. CO_{TC} has an estimated uncertainty for an individual measurement of 7–8% with standard deviations between ±2 and ±6% [*Yurganov et al.*, 2002]. AIRS Science Team Version 5 Level 2 daytime swaths are used here.

3 Analyses

3.1 Unique Fire Event

Figure 1a shows the location of all the active fires detected by MODIS Aqua and Terra for August 2010. We observe that FRP values greater than 500 Mwatts (yellow circles) are clustered southeast of Moscow (black star). This is a region of mixed and deciduous forest with a portion consisting of peatland (USSR State Forestry Committee, 1990). We focus on the southeast domain (cyan box, referred to as SE) covering 51-57°N and 37-50°E and tally the fire counts and FRP within that domain. Results are plotted in Figures 1a and 1b for June through August since 2003. We observe the following:

a) The fires are triggered earlier in 2010 than any previous year. On July 25th 2010, the fires ramp-up and sustain very high levels of activity and intensity through mid-August. By August 14th the fires begin to wane, while prior years show the fire products ramping up at this time and peaking later in the month.

b) Compared to prior years, the fires from late-July to mid-August 2010 are the most numerous and intense (two exceptions in FRP in 2008). Table 1 summarizes fire counts and FRP between July 25th and August 31st to include the 2010 fire event and seasonal fires that prior years show occurring throughout August. The statistics reveal exceptionally high values in 2010; FRP is an order of magnitude larger than previous years and the fire counts are almost doubled. The percentage increases in 2010 relative to the 2003-2009 mean are exceptionally high: 178% for fire count, and 309% for FNR.

At present, satellite measurements of fire activity are the best estimates of fire detection and strength [*Mottram et al.*, 2005; *Roy et al.,* 2008], however, it is important to keep the limitations of this data set in mind. In the vicinity of heavy clouds and very large fires the MODIS FRP may be less intense or not detected, resulting in a systematic low-bias in the measurements [*Giglio et al.,* 2006]. Ground fires, such as peat fires in our SE domain, generally do not produce sufficient heat to be detected by MODIS [*Roy et al.,* 2008]. Only subsets of fires are captured due to the relatively large viewing geometry, i.e. pixel sizes ranging from 1 km^2 at nadir to 4-5 km^2 at edge of the swath. Thus, although MODIS captures record fires over western Russia, the actual fire detected and intensity (in FRP) may be much higher.

Table 1. Combined MODIS Aqua and Terra fire counts and FRP in the SE domain [51-57°N, 37-50°E] between July 25th and August 31st per year.

Year	Fire Count	FRP [$\times 10^4$ Mwatt]
2010	**26,876**	**166.568**
2003-2009	9683	40.729
2009	6,784	33.270
2008	18,004	94.180
2007	11,206	49.842
2006	8,582	32.320
2005	12,873	43.224
2004	8,973	28.839
2003	1,358	3.428

3.2 Anomalous Surface Temperatures and Relative Humidity

Lau and Kim [2010] provides a thorough analysis of the synoptic weather patterns over western Russia that set-up the ideal conditions for the wildfires to thrive, spread and intensify for a prolonged period of time. Trajectory results from the NOAA HYSPLIT trajectory model [*Draxler and Rolph*, 2010] reveal the circulation pattern produced by this blocking event. Daily clusters of backward and forward trajectories initiated during the Aqua and Terra overpass time's, for the first week in August (during the height of the fires activity: see Fig. 1) from the Moscow city center (37.6°N, 55.7°E) at levels ranging from 0.5km up to 5km show a general clockwise motion indicative of a high-pressure system (not shown). Forward trajectories from clusters of fires SE of the city show transport of air toward Moscow. Surface temperate (T_{sfc}) and relative humidity (RH_{sfc}) anomalies from 12Z daily radiosonde measurements are plotted in Figure 2 at Moscow (red) and nearby stations (locations in Fig. 2c). Data were taken from the NOAA/Earth System Research Laboratory archive (http://www.esrl.noaa.gov/raobs/) going back to 1994. The daily anomalies are calculated by subtracting the 1994-2009 T_{sfc} and RH_{sfc} mean from their respective 2010 values. Focusing on the summertime period accentuates the anomalously high (positive) T_{sfc} and low (negative) RH_{sfc}, relative to 2010, associated with the blocking high-pressure system. From mid-June to mid-August the range of maximum T_{sfc} and minimum RH_{sfc} at these sites is 35-41°C and 9-25%, respectively. These anomalous meteorological parameters are coincident with the maximum time period of the fires, observed in Figure 1. Wind directions from the surface up to 700 hPa from late-July to early-August 2010 are predominantly from the SE quadrant (Fig. 2d, grey shaded). This further substantiates our claim that the smoke plumes reported over Moscow during the height of the fire activity (Fig. 1) originated from wildfires largely within the SE domain.

3.3 Exceptional Smoke and CO_{TC}

The OMI UVAI is a useful parameter for tracking absorbing aerosols (i.e. smoke) even in the presence of clouds [*deGraaf et al.*, 2005] and a few recent studies have used UVAI observations to link smoke plumes to biomass burning regions [*Fromm et al.*, 2005; *Torres et al.*, 2007; *Christopher et al.*, 2008]. The UVAI 3-day running mean over the Moscow domain (1°×1 ° area average around the city center) is plotted in Figure 3a measuring exceptionally high smoke (>> 1) in early August 2010 (red). Values greater than 1 rarely occur in previous years. Coincident with the start of the fire activity (Fig. 1), UVAI builds from July 25th, returning to mean values after mid-August. Between August 5th and 10th UVAI values > 2 and large1-sigma standard deviations > ±0.4 are observed, not seen in previous years. We do not show the UVAI within our SE domain because of significant under-sampling due to the row anomalies which, since 2009, affects almost half the OMI cross-track positions. The sparse data that are available qualitatively support the presence of elevated levels of UVAI in the SE domain.

The AIRS CO_{TC} over the Moscow and SE domains is plotted in Figure 3b. Again we see unprecedented levels of CO_{TC} peaking on August 7th of $37.1\pm5.1 \times10^{17}$ molec-cm^2 in the Moscow domain (red) and $39.1\pm4.4 \times10^{17}$ molec cm^2 in the SE domain (purple). We also observe elevated levels at the end of July 2006 (crosses) coincident with the

UVAI in Fig. 3a indicating another fire event, although short-lived compared to what we observe in 2010. Interestingly, as with the UVAI, the 1-sigma standard deviations are also large in both domains. The highest estimate occurs on August 1st at $\pm 7.4\times10^{17}$ molec-cm^2 and $\pm 5.4\times10^{17}$ molec-cm^2 over the Moscow and SE domains, respectively. CO_{TC} values over both domains are comparable in magnitude to that over Sumatra and Borneo, Indonesia during the 2006 El Niño wildfires (Fig. 3b, grey dotted and dashed lines, respectively). Exceptionally high values exceeding 30×10^{17} molec-cm^2 are observed during both events.

Table 2 highlights the record high levels of CO_{TC} and UVAI in 2010 (bold) relative to prior years during the August 1-18 peak period. CO_{TC} over Moscow and SE domains increases 53% and 58%, respectively, in 2010 relative to the 2003-2009 mean. UVAI over the Moscow domain increases an order of magnitude (~255%), relative to the 2005-2009 mean. Values of CO_{TC} in 2010 over both domains, including their 1-sigma standard deviations are similar to what we calculate over Sumatra and Borneo. During their peak period between October 10 and November 11, 2006 we estimate Sumatra CO_{TC} to be $34.7\pm3.9\times10^{17}$ molec-cm^2 and $34.9\pm5.3\times10^{17}$ molec-cm^2 over Borneo.

There is a dip in the CO_{TC} measurements over the Moscow domain on August 11th and 12th, followed by a second peak in mid-August (13th-18th). The UVAI also shows a slight secondary peak (Fig. 3a). Trajectory analyses on the 11th and 12th show winds from the SE domain transporting smoke eastward, away from Moscow, while the city receives air primarily from the south and southwest where fires continue to erupt and transport smoke (Fig. 1). However, CO_{TC} remains much higher relative to previous years.

After August 18th CO_{TC} and UVAI return to values typical of previous years. Noteworthy is the absence of elevated CO_{TC} in the SE domain in August from 2003 to 2009 concurrent with elevated active fires (Fig. 1). This may be due to the type of vegetation being burned in this region and/or that CO_{TC} is largely confined in the boundary layer where AIRS retrievals are less sensitive [*Yurganov et al.*, 2007]. Beside wildfires, peat fires may be contributing to the exceptionally high CO_{TC} in 2010. A significant portion of peat in Russia (60 Mt yr -1) is used as fuel [*Kolchugina and Vinson*, 1993]. In particular, peat fires are known to smolder for prolonged periods of time and emit large reservoirs of carbon, in the form for CO [*Immirzi et al.*, 1992; *Kasischke et al.*, 2005]. The degree of involvement of peat fires during this event and the altitude of the fire plumes prior to 2010 requires further study.

Table 2. August 1-18 mean per year of CO_{TC} [$\times10^{17}$ molec-cm^2] and UVAI [unitless] for the Moscow domain and SE domain (CO_{TC} only).

	SE Domain [51-57°N and 37-50°E]	Moscow Domain [1°×1° mean around the city center]	
Year	CO_{TC} ±1-σ	CO_{TC} ±1-σ	UVAI
2010	**32.43 ± 5.05**	**29.47 ± 2.62**	**1.49 ± 0.58**
2003-2009	20.48 ± 1.05	19.24 ± 0.58	2005-2009: 0.42 ± 0.19
2009	18.78 ± 0.98	17.34 ± 0.50	0.42 ± 0.13
2008	19.69 ± 1.04	17.91 ± 0.38	0.44 ± 0.23
2007	20.34 ± 1.01	18.69 ± 0.57	0.38 ± 0.18
2006	20.99 ± 1.19	19.62 ± 0.53	0.40 ± 0.23
2005	20.15 ± 0.88	18.64 ± 0.68	0.44 ± 0.20

2004	21.30 ± 1.19	20.58 ± 0.76	N/A
2003	22.09 ± 1.05	21.90 ± 0.65	N/A

4. Summary

EOS satellite multi-sensor data has enhanced our capability of tracking major atmospheric events, such as the 2010 Russian wildfires. Radiosondes stationed in western Russia measure anomalously high T_{sfc} (> 35°C) and low RH_{sfc} (< 25%) during the summer months. From late-July to mid-August 2010, record fires south and east of Moscow were observed by MODIS. The percentage increases in fire counts and FNR, relative to the 2003-2009 mean, are 178% and 309%, respectively. OMI UVAI over Moscow is an order of magnitude higher than previous years (255% increase). Likewise, AIRS CO_{TC} is 53% and 58% higher over the Moscow and SE domains, respectively. Exceptionally high CO_{TC} during the peak period of the Russian wildfires are comparable to what is observed during the 2006 El Niño wildfires over Sumatra and Borneo. Both events showed values exceeding 30×10^{17} molec-cm^2. After mid-August, MODIS fire activity drops well below what is typically seen in previous years, while UVAI and CO_{TC} return to mean values.

Acknowledgement: This work is supported by NASA's Atmospheric Chemistry, Modeling and Analysis, and Applied Sciences Air Quality Programs.

References

Alimov, Y.P., I.V. Golovikhin, L.B. Zdanevich, and I.V. Yunov (1989). Dynamics of forests under forest management organization regarding the main forest forming species in 1966-1988, *U.S.S.R State Forestry Committee*, pp. 159, Moscow.

Aumann H. H. et al. (2003), AIRS/AMSU/HSB on the Aqua Mission: Design, Science Objectives, Data Products, and Processing Systems, *IEEE Trans. Geo. Rem. Sens.*, 41, 253-264.

Christopher, S. A., P. Gupta, J. Haywood, and G. Greed (2008), Aerosol optical thicknesses over North Africa: 1. Development of a product for model validation using Ozone Monitoring Instrument, Multiangle Imaging Spectroradiometer, and Aerosol Robotic Network, *J. Geophys. Res.*, 113, D00C04, doi:10.1029/2007JD009446.

Crutzen, P. J. and M. O. Andreae (1990), Biomass Burning in the Tropics: Impact on Atmospheric Chemistry and Biogeochemical Cycles, *Science,* 250, 1669–1678.

deGraaf, M., P. Stammes, O. Torres, and R. B. A. Koelemeijer (2005), Absorbing Aerosol Index: Sensitivity analysis, application to GOME and comparison with TOMS, *J. Geophys. Res.*, 110, D01201, doi:10.1029/2004JD005178.

Draxler, R.R. and Rolph, G.D. (2010), HYSPLIT (HYbrid Single-Particle Lagrangian Integrated Trajectory) Model access via NOAA ARL READY Website (http://ready.arl.noaa.gov/HYSPLIT.php). NOAA Air Resources Laboratory, Silver Spring, MD.

Fromm, M., R. Bevilacqua, R. Servranckx, J. Rosen, J. P. Thayer, J. Herman, and D. Larko (2005), Pyro-cumulonimbus injection of smoke to the stratosphere: Observations and impact of a super blowup in northwestern Canada on 3–4 August 1998, *J. Geophys. Res.*, 110, D08205, doi:10.1029/2004JD005350.

Giglio L., J. Descloitres, C. O. Justice, and Yoram J. Kaufman (2003), An enhanced contextual fire detection algorithm for MODIS, *Remote Sens. Environ.*, 87, 273-282.

Giglio, L., I. Csiszar, and C. O. Justice (2006), Global distribution and seasonality of active fires as observed with the Terra and Aqua Moderate Resolution Imaging Spectroradiometer (MODIS) sensors, *J. Geophys. Res.*, 111, G02016, doi:10.1029/2005JG000142.

Immirzi CP, E. Maltby, and R. S. Clymo (1992), The Global Status of Peatlands and Their Role in Carbon Cycling. London: Wetlands Research Group, Friends of the Earth; 1992. Rep. No. 11.

Kasischke, E. S., E. J. Hyer, P. C. Novelli, L. P. Bruhwiler, N. H. F. French, A. I. Sukhinin, J. H. Hewson, and B. J. Stocks (2005), Influences of boreal fire emissions on Northern Hemisphere atmospheric carbon and carbon monoxide, *Global Biogeochem. Cycles*, 19, GB1012, doi:10.1029/2004GB002300.

Kolchugina, T.P. and T.S. Vinson (1993), Comparison of two methods to assess the carbon budget of forest biomes in the Former Soviet Union, *Water, Air, And Soil Pollution*, 70, 207-221.

Kaufman, Y., L. Remer, R. Ottmar, D. Ward, L. Rong-R, R. Kleidman, R. Fraser, L. Flynn, D. McDougal, and G. Shelton (1996), Relationship between remotely sensed fire intensity and rate of emission of smoke: SCAR-C experiment, in Global Biomass Burning, edited by J. Levine, pp. 685 – 696, MIT Press, Cambridge, Mass.

Lau W. K. M. and K. M. Kim, The 2010 Pakistan Flood and the Russia Heat Wave: Teleconnection of Extremes, *Nature Geosciences*, submitted, 2010.

Mottram G. N., M. J. Wooster, H. Balster, C. George, F. Gerrard, J. Beisley (2005), The use of MODIS-derived fire radiative power to characterise Siberian boreal forest fires, *Proceedings of the 31st international symposium on remote sensing of environment*, St. Petersburg, Russian Federation, 20–24 June 2005.

Olson, J. S., J. A. Watts, and L. J. Allison (1983). Carbon in live vegetation of major world ecosystem, ORNL-5862, Oak Ridge.

Roy, D.P., L. Boschetti, C. O. Justice, and J. Ju (2008), The Collection 5 MODIS Burned Area Product - Global Evaluation by Comparison with the MODIS Active Fire Product, *Remote Sens. Environ.*, 112, 3690-3707.

Torres, O., A. Tanskanen, B. Veihelmann, C. Ahn, R. Braak, P. K. Bhartia, P. Veefkind, and P. Levelt (2007), Aerosols and surface UV products from Ozone Monitoring Instrument observations: An overview, J. Geophys. Res., 112, D24S47, doi:10.1029/2007JD008809.

USSR State Forestry Committee (1990), *Forest Fund of the USSR,* Vol 1,1005 pp., Moscow.

Yurganov, L. N., W. W. McMillan, A. V. Dzhola, E. I. Grechko, N. B. Jones, and G. R. van der Werf (2008), Global AIRS and MOPITT CO measurements: Validation, comparison, and links to biomass burning variations and carbon cycle, *J. Geophys. Res.,* 113, D09301, doi:10.1029/2007JD009229.

Figure 1. Combined Aqua and Terra fire counts and FNR over the SE domain are plotted in (a) and (b), respectively. Map inset in (a) of Aqua and Terra fire counts (red circles). Yellow circles indicate FNR > 500 Mwatts. Star marks the location of Moscow. The cyan box defines the SE domain covering 51-57°N and 37-50°E.

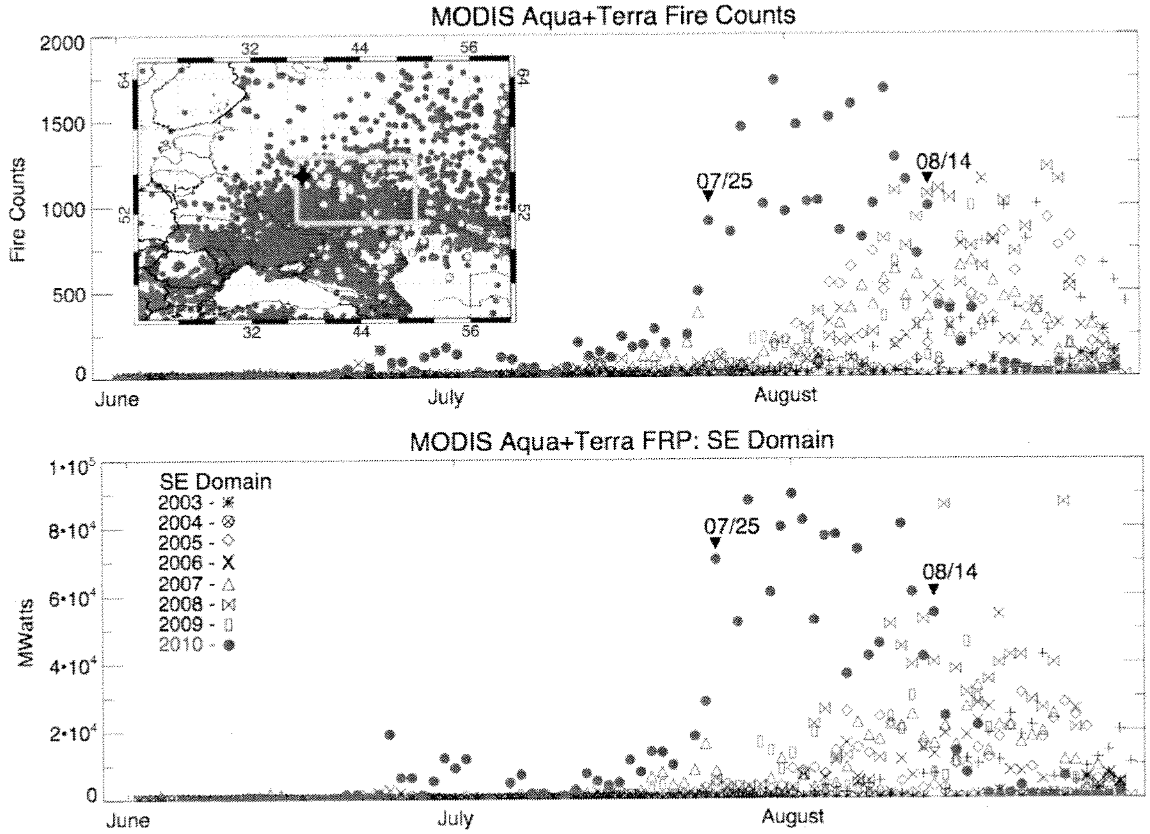

Figure 2. (a) T_{sfc} and (b) RH_{sfc} anomalies. Radiosonde locations, including symbol legend for (a) and (b) are mapped in (c). Wind directions in July and August 2010 are shown in (d) at the surface (red), 850hPa (blue), and 700hPa (green). Grey shading highlights the southeast quadrant.

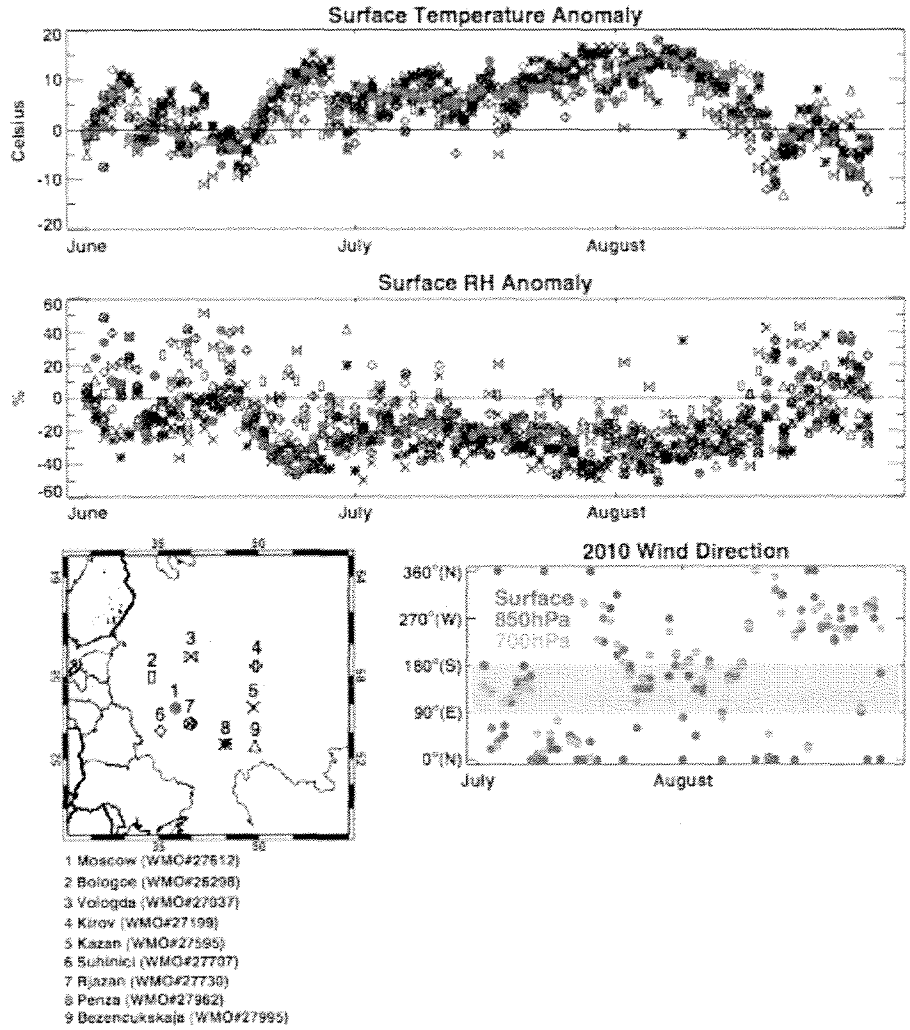

Figure 3. (a) UVAI plotted per year over the Moscow domain between June and August. 2010 is highlighted in red. CO_{TC} in (b) plotted similar to (a), also including the SE domain (purple). The 1-σ standard deviations are plotted for 2010 only in grey shading. Sumatra [96-107°E, 7°S-5°N] (grey dotted) and Borneo [109-119°E, 5°S-5°N] (grey dashed) are overlaid in (b) for September - November 2006.